

THE EFFECT OF SWIRLING FLOW ON PIPE FRICTION LOSSES

by
Carl R. Janik
Mahadevan Padmanabhan

Research Sponsored by
Yankee Atomic Electric Company
Public Service Company of New Hampshire

ARL ALDEN RESEARCH LABORATORY
WORCESTER POLYTECHNIC INSTITUTE

February 1980

26-81/M296KF

8112010238 811127
PDR ADDCK 05000443
A PDR

THE EFFECT OF SWIRLING FLOW
ON PIPE FRICTION LOSSES

by

Carl R. Janik
Mahadevan Padmanabhan

Research Sponsored by
Yankee Atomic Electric Company
Public Service Company of New Hampshire

George E. Hecker, Director
ALDEN RESEARCH LABORATORY
WORCESTER POLYTECHNIC INSTITUTE
HOLDEN, MASSACHUSETTS

February 1980

ABSTRACT

Results obtained from tests conducted on the Seabrook Containment Sump model at the Alden Research Laboratory (ARL) revealed small amounts of swirling flow within the sump suction pipes. The effect that swirling flow has on pipe friction losses, and in turn on the Net Positive Suction Head requirements of the Emergency Core Cooling Recirculating pumps, was not understood; therefore, it was decided beneficial to conduct a separate study in order to determine the effects of swirling flow on pipe friction losses. The study was conducted at ARL and sponsored by Yankee Atomic Electric Company.

An experimental facility was constructed consisting of: 34 ft of 10 inch diameter pipe containing a swirl generator; a series of pressure taps; a flow meter; and capabilities for placing a vortimeter either upstream or downstream of the pressure taps. The system had the ability of producing swirling flow from set swirl generator values of from 0° to 40° and for Reynolds numbers in the range of 1.0 to 3.5×10^5 .

Preliminary tests of the system revealed that the discharge coefficient of the orifice type flowmeter was dependent on the set swirl angle. There was an approximate 5% increase in the discharge coefficient for 40° swirling flow compared to non-swirling flow. Results indicated that swirling flow had practical effects on the frictional losses; for example, friction losses in the pipe due to swirling flow with 20° swirl vane settings were approximately 40% higher than those for non-swirling flow, at the corresponding Reynolds numbers. Swirl decay was found to vary with swirl angle and also to depend on Reynolds numbers and the results obtained were consistent with the findings of other researchers.

TABLE OF CONTENTS

	<u>Page No.</u>
ABSTRACT	i
TABLE OF CONTENTS	ii
INTRODUCTION	1
SWIRL ANGLE	2
TEST FACILITY	3
TEST PROGRAM	5
RESULTS	6
CONCLUSIONS	8
ACKNOWLEDGEMENTS	9
REFERENCES	10
PHOTOGRAPHS	
FIGURES	

INTRODUCTION

Hydraulic model tests on a 1:4 scale model of the Seabrook Nuclear Power Station containment sump, conducted at the Alden Research Laboratory (ARL) of Worcester Polytechnic Institute (WPI) (1) showed the existence of small amounts of swirl in the flow within the suction pipes when operating with partially blocked vertical sump screens even though no strong free surface vortices of concern were observed. The swirl angles, as indicated by a vortimeter, were mostly less than 5 degrees, which may be considered too small to cause pump impeller vibrations. However, realizing the necessity of accurately evaluating the available Net Positive Suction Head (NPSH) for the recirculating pumps, the effect of this swirl on the entrance loss and pipe friction loss was of concern. Determination of total intake losses, including entrance losses, was a part of the sump model study (1). However, it was decided to conduct a separate investigation on the effect of swirl on pipe friction losses so that differing degrees of swirling flow could be established to provide more general information on the subject. This was particularly desired since swirling flow in suction pipes could also be caused by combined bends in piping systems as well as from any rotational flow in the sump (2).

Although several studies have been completed on swirling flow in pipes, most of the research has been conducted at small pipe diameters and high swirl angles (3, 4, 5, 6). These studies are not representative of the conditions that exist in a reactor sump where pipe diameters are large, flowrates are high, and swirl angles are relatively small, less than 15°. Therefore, specific results concerning the effect of low intensity swirling flow on the frictional losses in sump suction pipes are not readily available for a designer, and the need for an additional study is evident.

A separate experimental setup was constructed at the ARL, and considering the usefulness of the study to the design of the Seabrook ECCS system, the project was sponsored by the Yankee Atomic Electric Company (YAEC). In

order to accurately determine the effect of various degrees of swirling flow on the pipe friction factor, a systematic test program was set up, whereby both the degree of swirl and the flowrate could be varied within a 10 inch pipe. The degree of swirl was varied using a four vaned swirl generator, enabling an accurate and easy method of setting the swirl angle.

SWIRL ANGLE

Swirling flow in a pipe can be considered as a combination of vortex motion and axial motion along the pipe axis, which means the existence of axial components and tangential components of velocities at any point in the flow field. For the problem of concern in the present investigation, the swirling flow is turbulent, incompressible, and steady. Along the length of the pipe the swirl level decays and the velocity and static pressure distributions change with axial position along the pipe.

For the present study, the rotational speed, ω , of a vortimeter which consists of a vaned rotor containing four blades, was used for swirl measurements. The swirl level was calculated using the measured ω values and expressed mainly as an indicated swirl angle θ defined as (7):

$$\theta = \tan^{-1} \frac{\omega d/2}{u} \quad (1)$$

where d is the internal diameter of the pipe and u is the average axial (cross-sectional) velocity of the flow. Equation (1) can be rewritten in terms of vortimeter rotations, n per second:

$$\theta = \tan^{-1} \frac{\pi n d}{u} \quad (2)$$

The use of the term ω or n to indicate swirl level was considered convenient and easily understandable. A more commonly used fluid mechanics term, the angular momentum of flux, K , could be derived using the rotational speed ω of the vortimeter (6), as given by:

$$K = \pi \rho u r^2 \omega (r^2 + r_i^2)/2 \quad (3)$$

where ρ is the water density, r is the pipe radius, and r_i is the rotor hub radius of the vortimeter. Equation (3) assumes negligible losses and rigid body motion. With the axial momentum expressed as $M = \pi \rho u^2 d^2/4$, the swirl level could then be defined by a parameter K/Md .

Combining Equations (1) and (3), a relationship between θ and K could be obtained as,

$$\theta = \tan^{-1} \left[\frac{K}{\pi \rho u^2 r (r^2 + r_i^2)/2} \right] \quad (4)$$

The swirl decay between two locations in the pipe at an axial distance of Δx apart has been shown by many investigators (4, 6, 8) to follow an exponential function which could be defined as,

$$\frac{K}{K_0} = e^{-\beta \Delta x/d} \quad (5)$$

where K_0 and K are the upstream and downstream angular momentum fluxes, respectively, a distance Δx apart, and β is a decay parameter which depends on the Reynolds number, $Re = \frac{u d}{\nu}$, as well as the upstream swirl level indicated by K_0/Md .

TEST FACILITY

The test facility used in this study is shown in Figure 1 and Photograph 1. Water was drawn from a sump through a 12 inch line by a 10 HP pump. The flow then passed through a 12" x 10" reducer and a series of flow straighteners, initially consisting of two perforated plates separated by one pipe diameter. In order to ensure a flat velocity profile in the pipe, a pitometer traverse was obtained downstream of the straighteners. The initial velocity traverse showed a higher velocity region away from the center which was remedied by

placing a ring, constructed of perforated plate, between the plates of the flow straightener, thereby directing the flow towards the center of the pipe. The velocity traversing points and the final velocity profile obtained are shown in Figure 2.

The swirl generator was located 8 diameters downstream of the flow straightener and, as previously stated, consisted of 4 adjustable vanes. The 4 vanes were 90° apart in the circumferential direction, one diameter long and occupied 90% of the diameter of the pipe. Vane angles were adjustable from 0° to 40° with respect to the axis of the pipe, and had an attainable setting accuracy of $\pm 1/2^\circ$. The swirl generator is shown in Photograph 2.

A series of 10 static pressure taps were located starting 11 diameters downstream of the swirl generator. The pressure taps were set one diameter apart and connected to air-water manometer tubes (Photograph 3). In order to record the piezometric head from each tap at a particular instant of time, photographic documentation of all the taps was made and measurement of the piezometric head was obtained from the photograph.

Both upstream and downstream of the pressure taps, spool pieces were provided for the placement of a cross-vaned vortimeter. Photograph 4 shows the vortimeter with its 4 perpendicular vanes, each 4 inches long and 8 inches wide, attached to a rotor hub of radius 0.9 inches. The revolutions per any desired period of time were counted using an optical sensor and an electronic counter. To keep the pipe length of the system constant, which was necessary in order to obtain accurate swirl decay data, a blank spool section equal in length to the vortimeter was placed in the space not occupied by the vortimeter. To ensure that the vortimeter did not affect the pressure gradient measurements, readings of the gradeline were taken while the vortimeter was in the downstream position.

An orifice meter, coupled to a differential manometer, and located downstream of the pressure taps, provided a means of monitoring flow through the system. Since the orifice meter was located downstream of the swirl generator, it was necessary to establish the effect of swirling flow on the flow meter discharge coefficient for various swirl angles. In order to establish this, the section of the facility from the swirl generator to the meter was removed and calibrated in ARL facilities. An accuracy of $\pm 0.25\%$ is expected for flow measurements.

In order to be representative of large scale reactor sump models, a relatively large flowrate was needed, although the maximum flowrate attained in the model was limited to 2.5 cfs. A control valve was located downstream of the orifice plate and was used to vary the flow through the system. Flow was routed back to the sump, thus completing the cycle.

TEST PROGRAM

In order to accurately determine the effect of swirl on the pipe friction losses, a test program was set up using six swirl angles, 0, 6, 10, 20, 30, and 40 degrees, each tested at 12 flowrates of between 1 and 2.5 cfs. At each swirl angle and flowrate, pressure gradients for 9 diameters of pipe length were obtained. Vortimeter readings were obtained both upstream and downstream of the pressure taps for the above swirl angles and also for 15, 25, and 35 degrees.

The friction factor for the specified pipe length was obtained from the Darcy-Weisbach formula:

$$f = \Delta h \left(\frac{d}{L} \right) \left(\frac{2g}{u} \right) \quad (6)$$

where

- f = calculated friction factor
- Δh = measured pressure differential over 9d
- d = diameter of pipe, 10.0 inches
- L = nine diameters length = 9d
- u = average velocity calculated from $u = Q/A$
 with Q measured by the orifice meter and $A = \pi d^2/4$

An average pressure gradient for the 9 diameter length was obtained from a least squares fit through individual readings taken at one diameter spacings.

Knowing the number of rotations of the vortimeter, n, the indicated swirl angle, θ was obtained from Equation (2). By determining the indicated swirl angle at the two vortimeter locations, a percent swirl decay over 17 pipe diameter lengths could be determined from:

$$\text{Percent Swirl Decay} = \frac{\theta_{\text{up}} - \theta_{\text{down}}}{\theta_{\text{up}}} \times 100 \quad (7)$$

where θ_{up} and θ_{down} are the measured swirl angles upstream and downstream of the pressure taps, respectively. Decay rates were determined for all flows and swirl angles. The values of the angular momentum fluxes were also calculated using Equation (3) and the decay parameter β was evaluated using Equation (5). As β is a function of R_e and K_o/MD , curves were obtained for β versus R_e with K_o/MD approximately constant and β versus K_o/MD with R_e approximately constant. An average K value (K_{av}) was obtained from Equation (5) as $K_{\text{av}} = \frac{1}{L} \int_0^L K \, dx$, and K_{av} was used to denote the average swirl level over the pipe length of L ($L = 9d$ for friction measurements). θ_{av} was derived from K_{av} using Equation (4). This enabled the plotting of percentage increase in friction loss due to swirl versus θ_{av} curves, for constant Reynolds numbers. These curves may be used by designers to predict approximately the frictional losses for pipes with swirling flows, if the approximate swirl angles and the frictional losses for non-swirling flow at the Reynolds number of interest are known.

RESULTS

As shown in Figure 2, a fully developed velocity profile was obtained upstream of the swirl generator by proper flow straightening devices. No residual swirl was indicated by the vortimeter for a zero setting on the swirl generator.

The results of the orifice meter calibration are shown in Figure 3, in which the angles set at the swirl generator (θ_{set}) are indicated to denote the swirl level. At the largest swirl angle tested, $\theta_{\text{set}} = 40^\circ$, the presence of swirl increased the discharge coefficient by approximately 5% for all flow-rates tested. The effect of smaller swirl angles was progressively less, as shown in Figure 3.

In order to verify the operation of the swirl generator, vortimeter readings were taken at the upstream location and transformed into indicated swirl angles using Equation (2). The indicated θ values (θ_I) were then compared to

to the set readings (θ_{set}) on the generator. As shown in Figure 4, for set swirl angles less than approximately 15° , the indicated swirl angle is less than the set swirl and for larger set swirl angles, the indicated swirl was seen to be slightly greater than the set swirl. This fact could be caused by adverse flow patterns past the swirl generator involving flow separation at the vanes.

Because of the swirl decay, the pressure gradient in a pipe with swirling flow might not be linear. However, in this investigation over the nine pipe diameter length, the gradient was assumed to be linear since the non-linearity could not be accurately defined due to experimental limitations (piezometric heads could be measured only to an accuracy of ± 0.005 ft). Equation (6) was used to calculate an equivalent friction factor f .

Results of the effect of swirl on the friction factor are shown in Figure 5. As shown in the figure, the friction factor increases substantially with set vane angle. The impact that these results would have on calculating pipe friction losses can be seen more clearly in Figure 6. In this figure, the percentage increase in the friction losses for a particular average swirl angle, θ_{av} , compared to zero degree swirl, is plotted against the average swirl angle for the region of no R_e dependence (i.e., $R_e > 2.0 \times 10^5$). At the swirl angles of interest for the Seabrook sump (θ_{av} up to 5 degrees), an increase of up to 10% in the friction losses over that for non-swirling flow can be expected.

Figure 7 presents data for swirl decay over 17 pipe diameters. As seen in the figure, there is a higher decay rate for small swirl angles and a lesser decay, 20%, for larger swirl angles. Thus, in the range of interest (up to 20 degrees), more than 60% of the swirl could be expected to decay in 17 pipe diameters. Dependence of decay rates on swirl intensity and Reynolds number was also observed by other researchers (5, 6).

Figure 8 shows the variation of the decay parameter, β , with the pipe Reynolds number for various set swirl generator angles. β is more or less independent of R_e for R_e greater than 2×10^5 and swirl angles greater than 25° . β increases with decreasing R_e for a particular set swirl generator vane angle (θ_{set}). Also given in Figure 8 is a comparison of the range of (K_o/Md) for a given set swirl generator angle. This Reynolds number dependence of β is consistent with the results in references (5, 6).

CONCLUSIONS

The following conclusions can be drawn from this study:

1. Swirling flow has an effect on the performance of an orifice meter. At the highest swirl angle of 40 degrees (swirl generator vane setting) used in this study, the orifice meter discharge coefficient increased by about 5 percent compared to the same flowrate with no swirl. For small indicated swirl angles (less than 10 degrees), the effect of swirl on orifice meter performance was found to be negligible (less than 1 percent).
2. The effect of swirling flow on the friction loss is dependent on swirl intensity. For an average indicated swirl angle of 5 degrees (normally encountered in suction pipes due to inlet rotational flow), the increase in the frictional loss would be approximately 15% compared to that for non-swirling flow at the same Reynolds number. For a higher swirl angle, the increase in friction factor would be greater.
3. Swirl decay with distance is a function of Reynolds number as well as initial swirl angle. However, for R_e greater than 2×10^5 , swirl decay is more or less only dependent on the initial swirl level for the larger swirl levels tested. The decay parameter, β , decreased from 0.056 to 0.014 for increasing swirl generator vane angles of 20 to 40 degrees (or for K/Md values from 0.10 to 0.37) for R_e greater than 2×10^5 .

ACKNOWLEDGEMENTS

The help provided by all members of the staff at the Alden Research Laboratory in conducting the study is acknowledged. Particular thanks are due to Professor George E. Hecker for his helpful suggestions during this investigation.

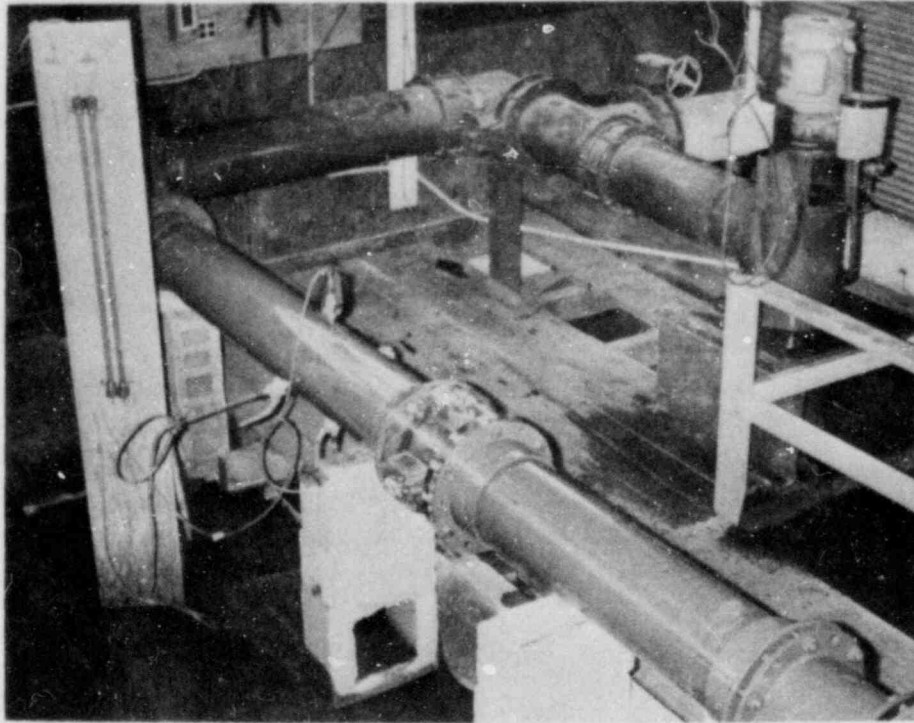
Special mention must be made of the work done by Messrs. J. Noreika and M. Majcher who contributed greatly to the design and construction of the experimental setup and carried out the experiments with considerable care.

Financial support for this research was provided by Yankee Atomic Electric Company, and their interest and support are greatly acknowledged.

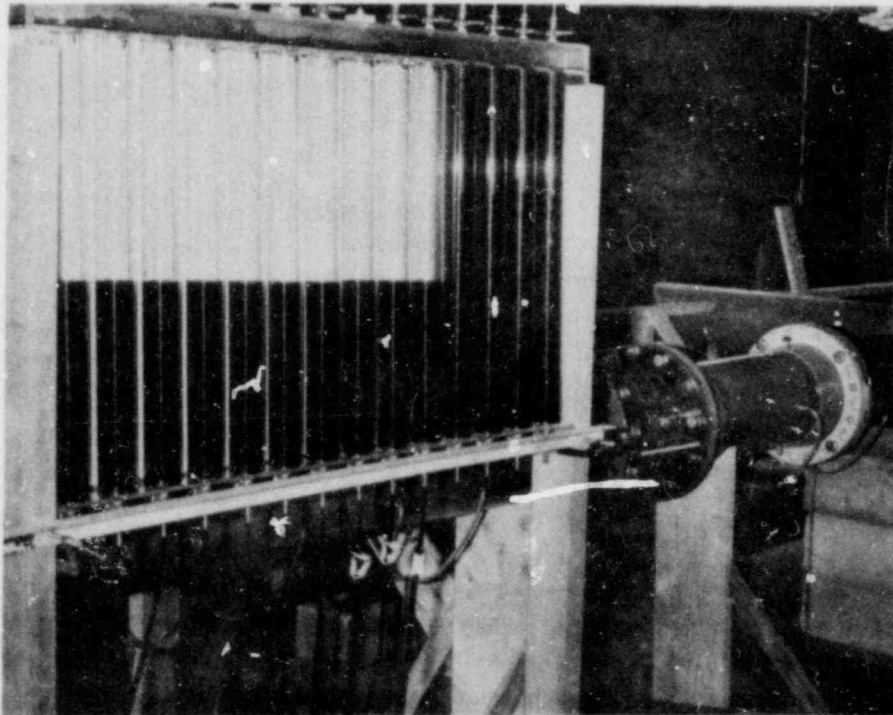
REFERENCES

1. Padmanabhan, M., "Investigation of Vortexing and Swirl Within a Containment Recirculation Sump Using a Hydraulic Model - Seabrook Nuclear Power Station," ARL Report, May 1979.
2. March, P.A., and Noreika, J.F., "Investigation of Swirl and Axial Velocity Distribution in Suction Piping," ARL Report No. 127-77/M220AF, August 1977.
3. Kreith, F., and Sonju, O.K., "The Decay of a Turbulent Swirl in a Pipe," Journal of Fluid Mechanics, 22, 1965.
4. Youssef, T.E.A., "Some Investigations on the Rotating Flow With a Recirculating Core in Straight Pipes," ASME Paper 66-WA/FE-36, 1966.
5. Rochino, A.P., and Lavin, Z., "Analytical Investigation of Incompressible Turbulent Swirling Flow in Pipes," NASA CR-1169, 1968.
6. Baker, D.W., and Sayre, C.L., "Decay of Swirling Turbulent Flow of Incompressible Fluids in Long Pipes," Flow - Its Measurement and Control in Science and Industry, 1974.
7. Hattersley, R.T., "Hydraulic Design of Pump Intakes," Journal of Hydraulics Division, ASCE, November 1974.
8. Davis, R.W., et al., "Numerical Solutions for Turbulent Swirling Flow Through Target Meters," ASME Winter Annual Meeting, San Francisco, California, August 1979.

PHOTOGRAPHS

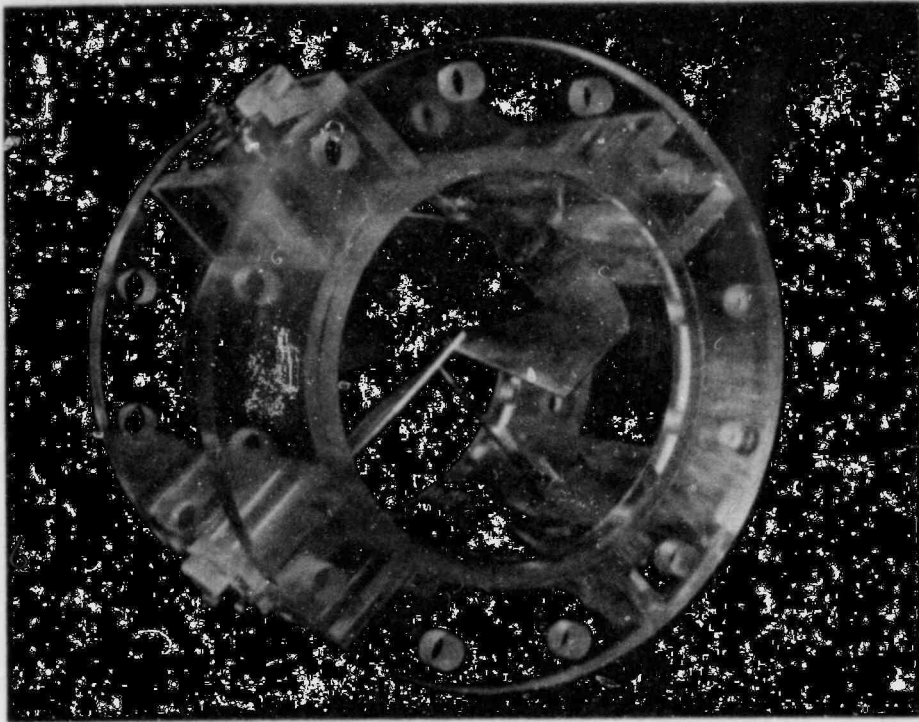


a) Upstream of Pressure Taps

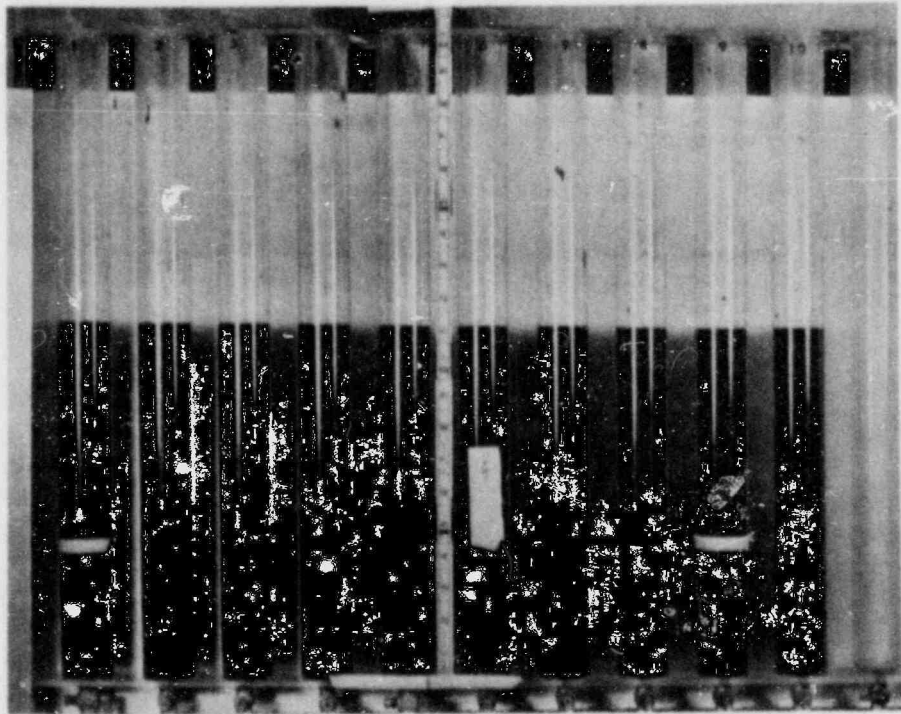


b) Downstream of Pressure Taps

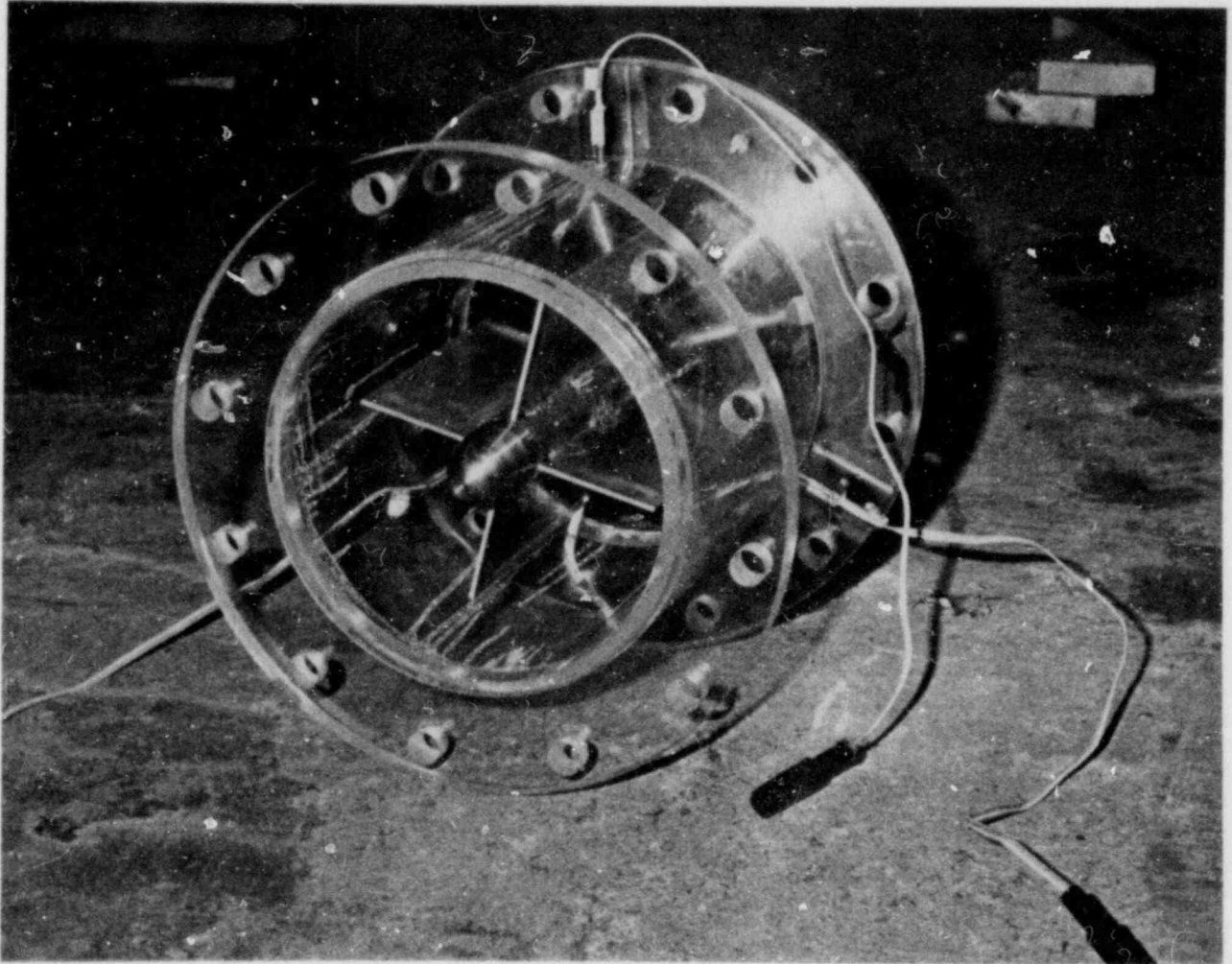
Photograph 1 Experimental Set-Up



Photograph 2 Swirl Generator



Photograph 3 Typical Pressure Gradient
 $\theta_{\text{set}} = 10^\circ$; $Re = 2.15 \times 10^5$



Photograph 4 Vortimeter Used for Swirl Measurements

FIGURES

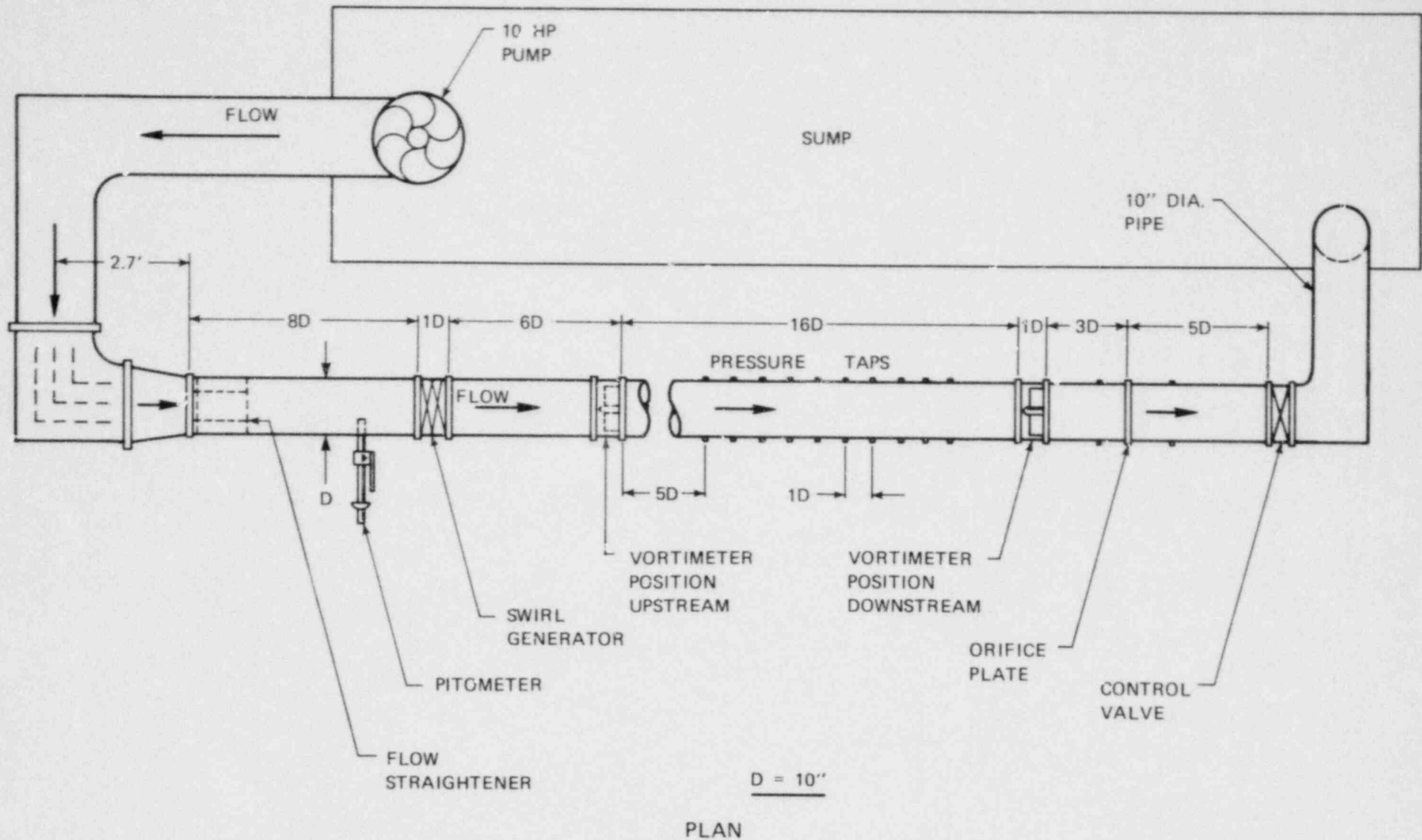
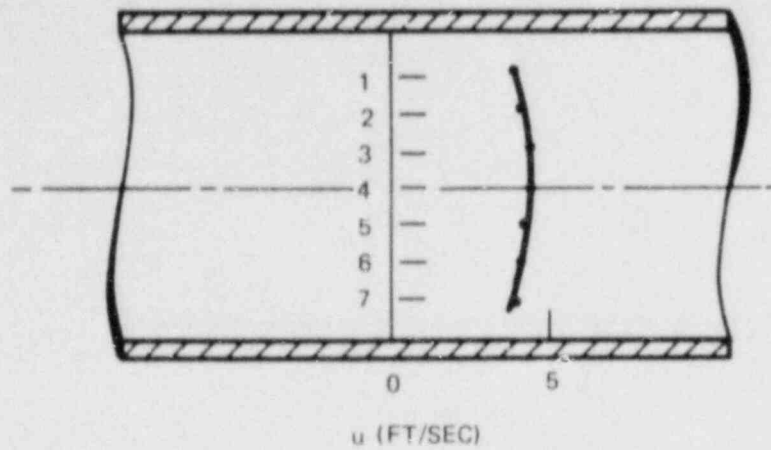
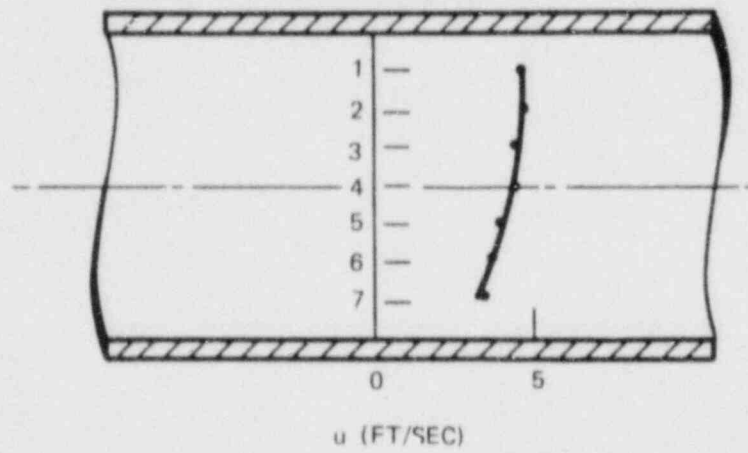


FIGURE 1 EXPERIMENTAL FACILITY



a) VERTICAL TRAVERSE



b) HORIZONTAL TRAVERSE

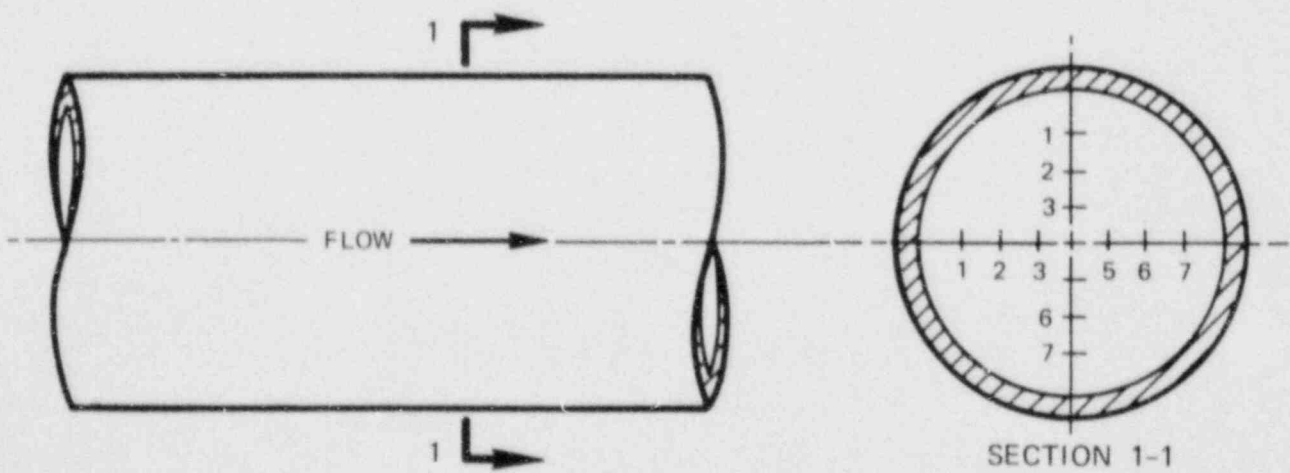


FIGURE 2 PITOMETER TRAVERSING POINTS AND VELOCITY PROFILES

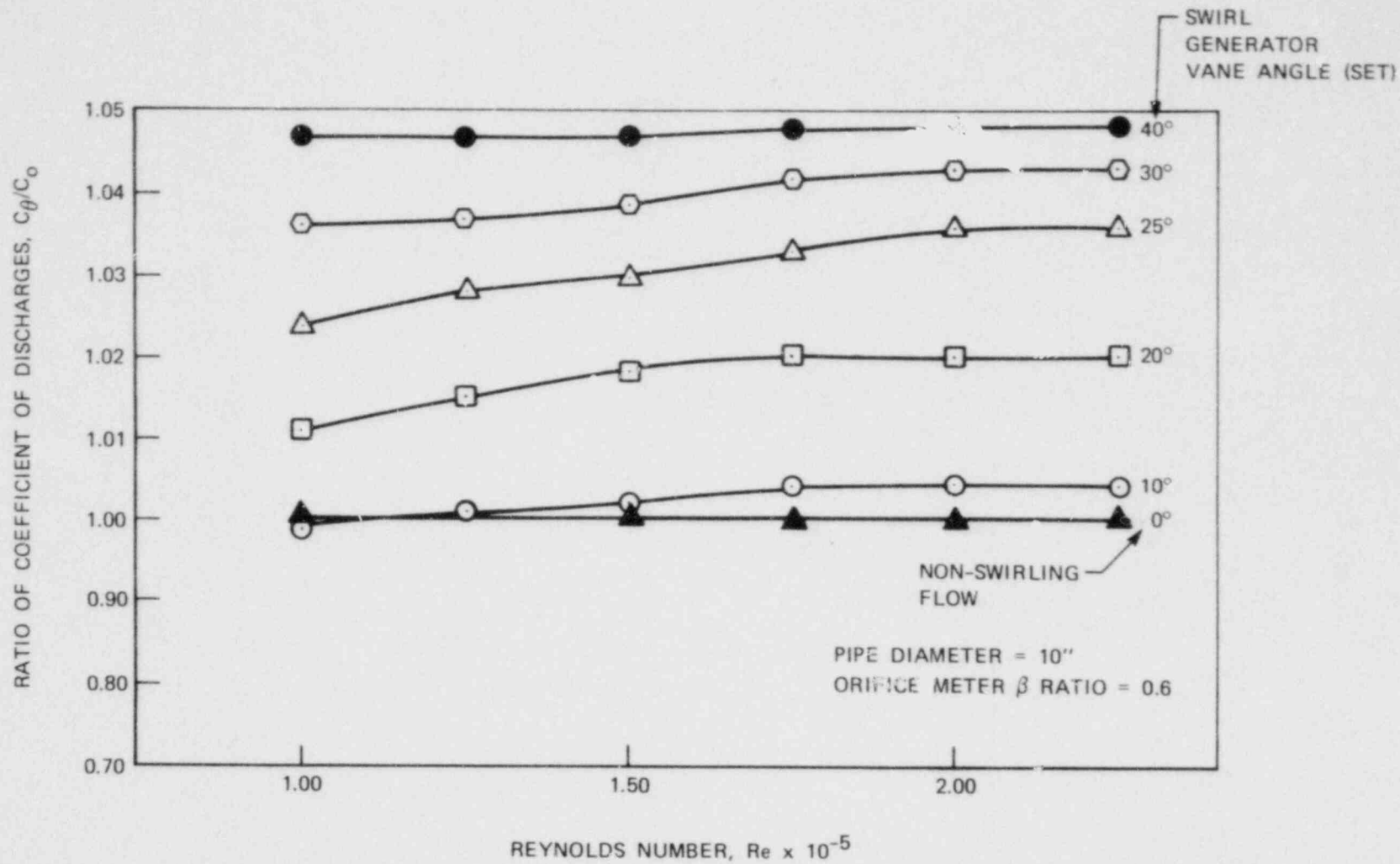


FIGURE 3 ORIFICE METER CALIBRATION WITH SWIRLING FLOW

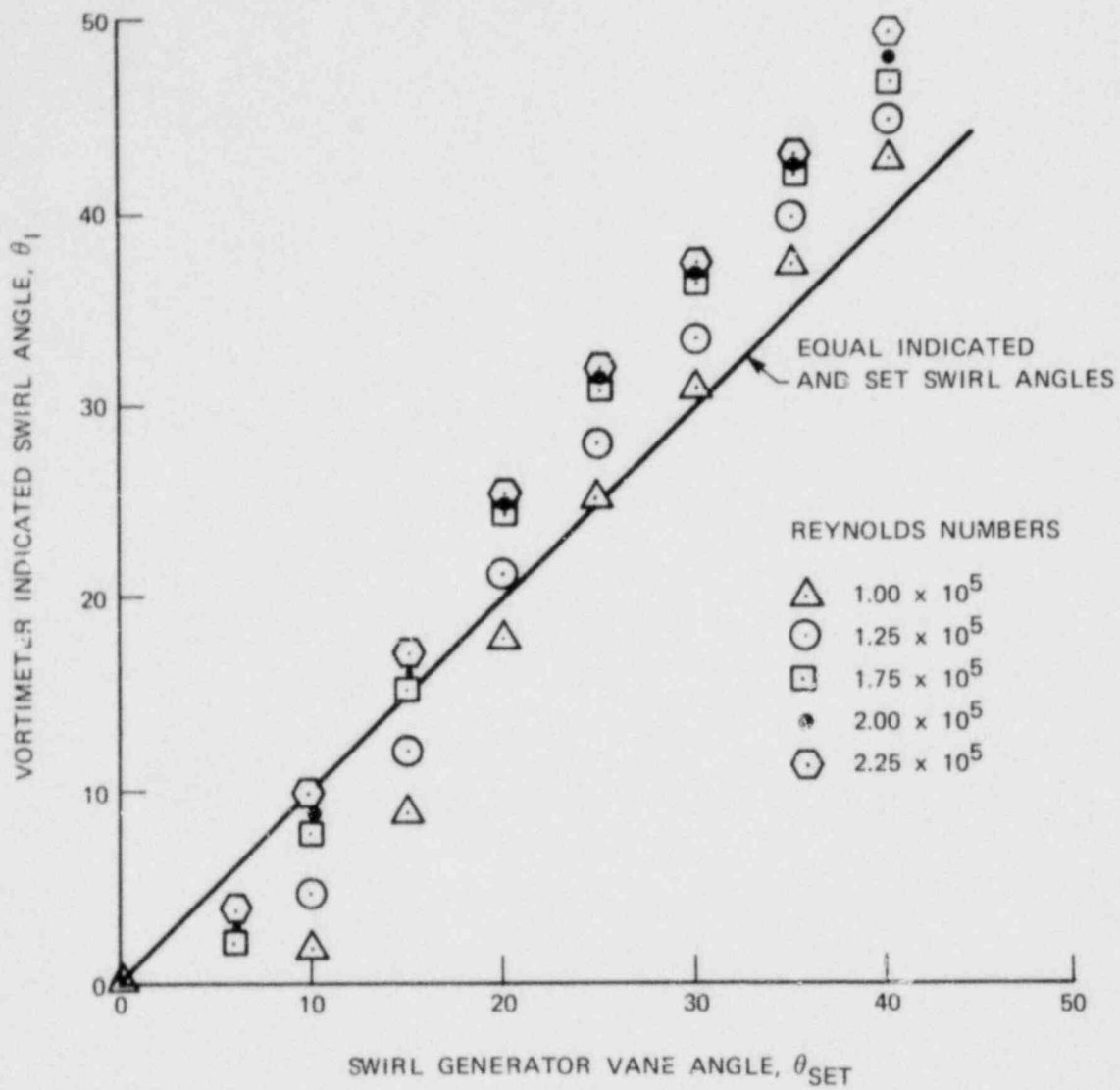


FIGURE 4 VORTIMETER COMPARISON OF INDICATED SWIRL ANGLE UPSTREAM LOCATION VERSUS SWIRL GENERATOR VANE ANGLE

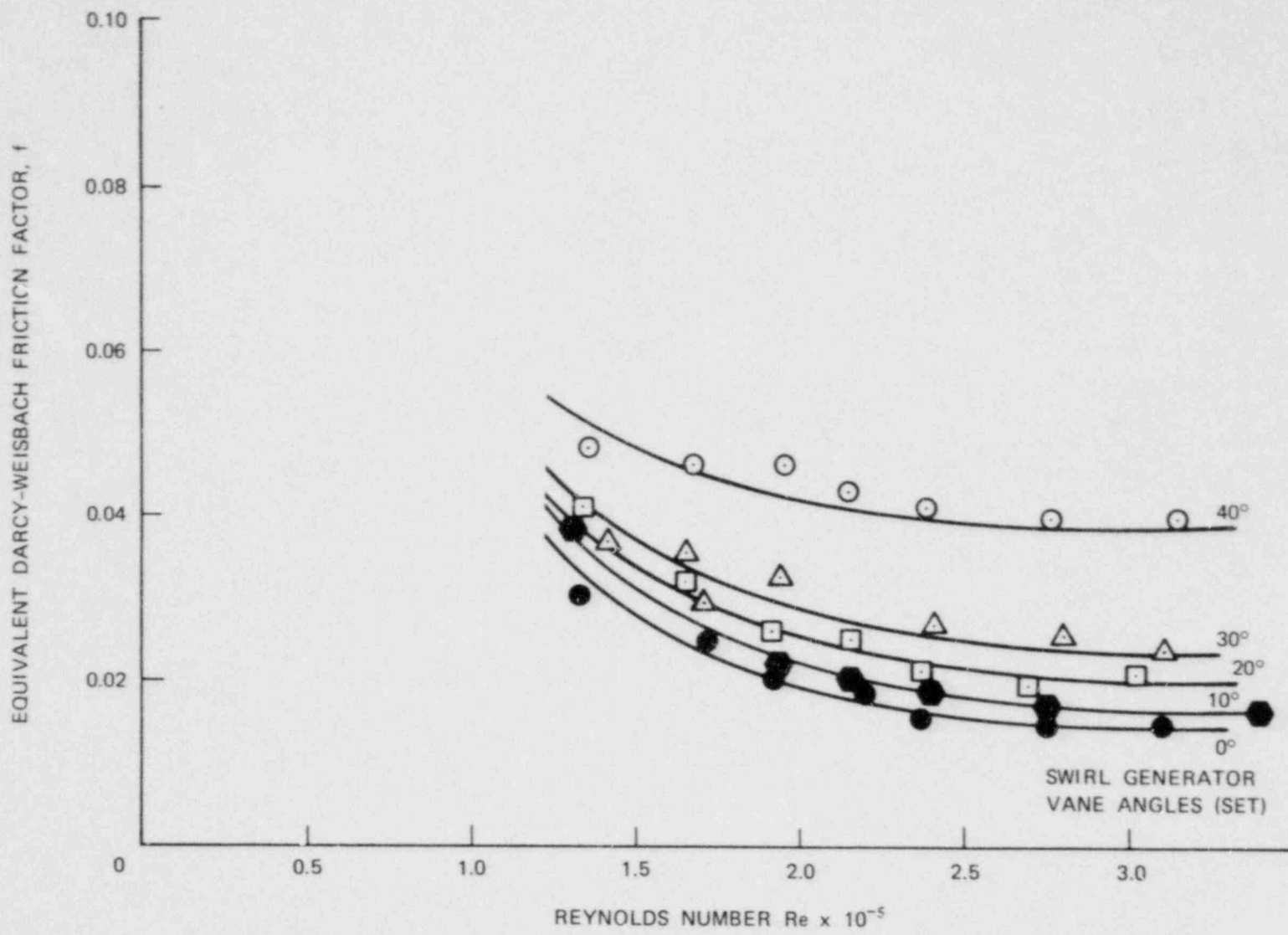


FIGURE 5 FRICTION FACTOR VERSUS REYNOLDS NUMBER FOR VARIOUS SWIRL ANGLES

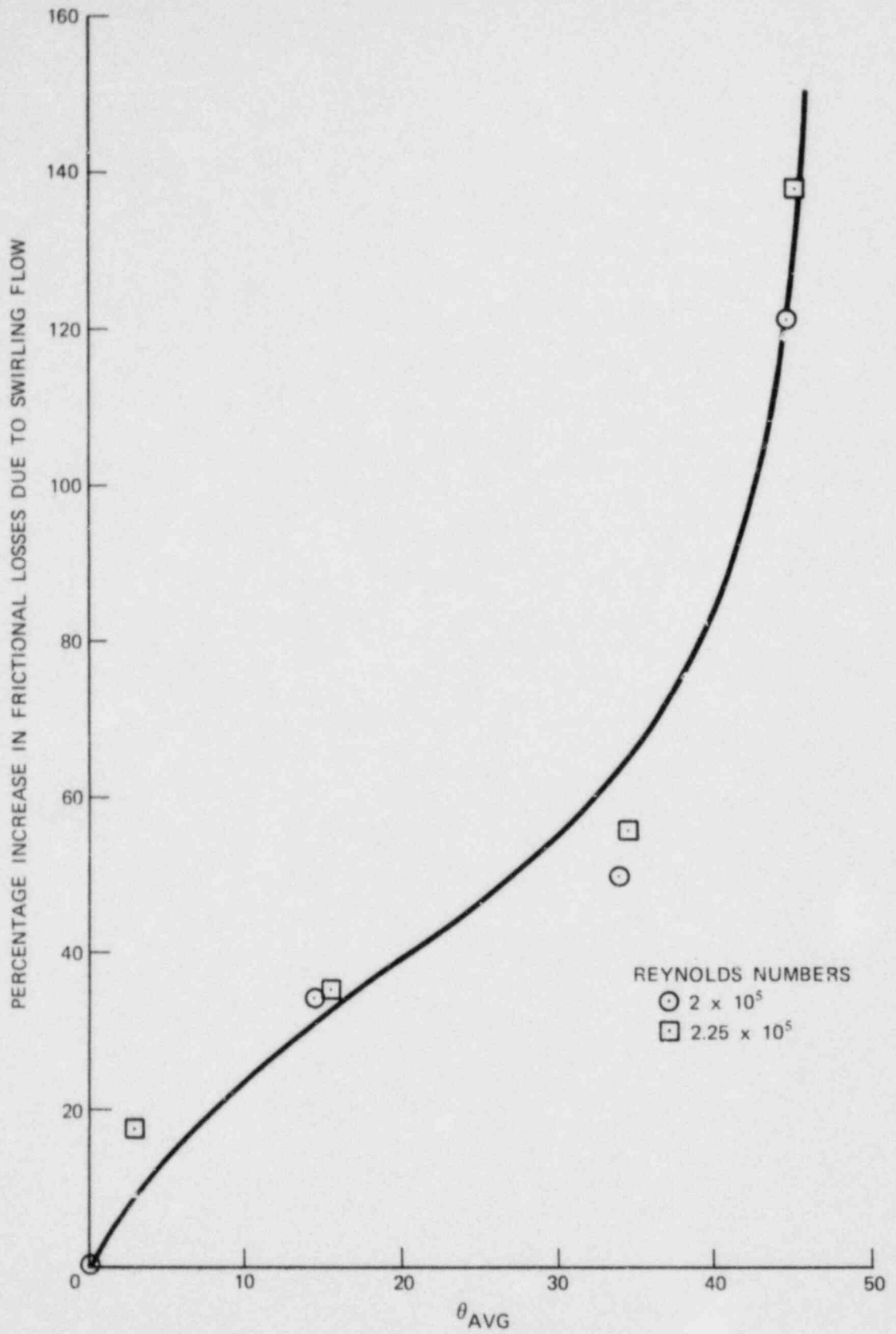


FIGURE 6 PERCENT INCREASE IN THE FRICTIONAL LOSSES FOR AVERAGE INDICATED SWIRL ANGLES

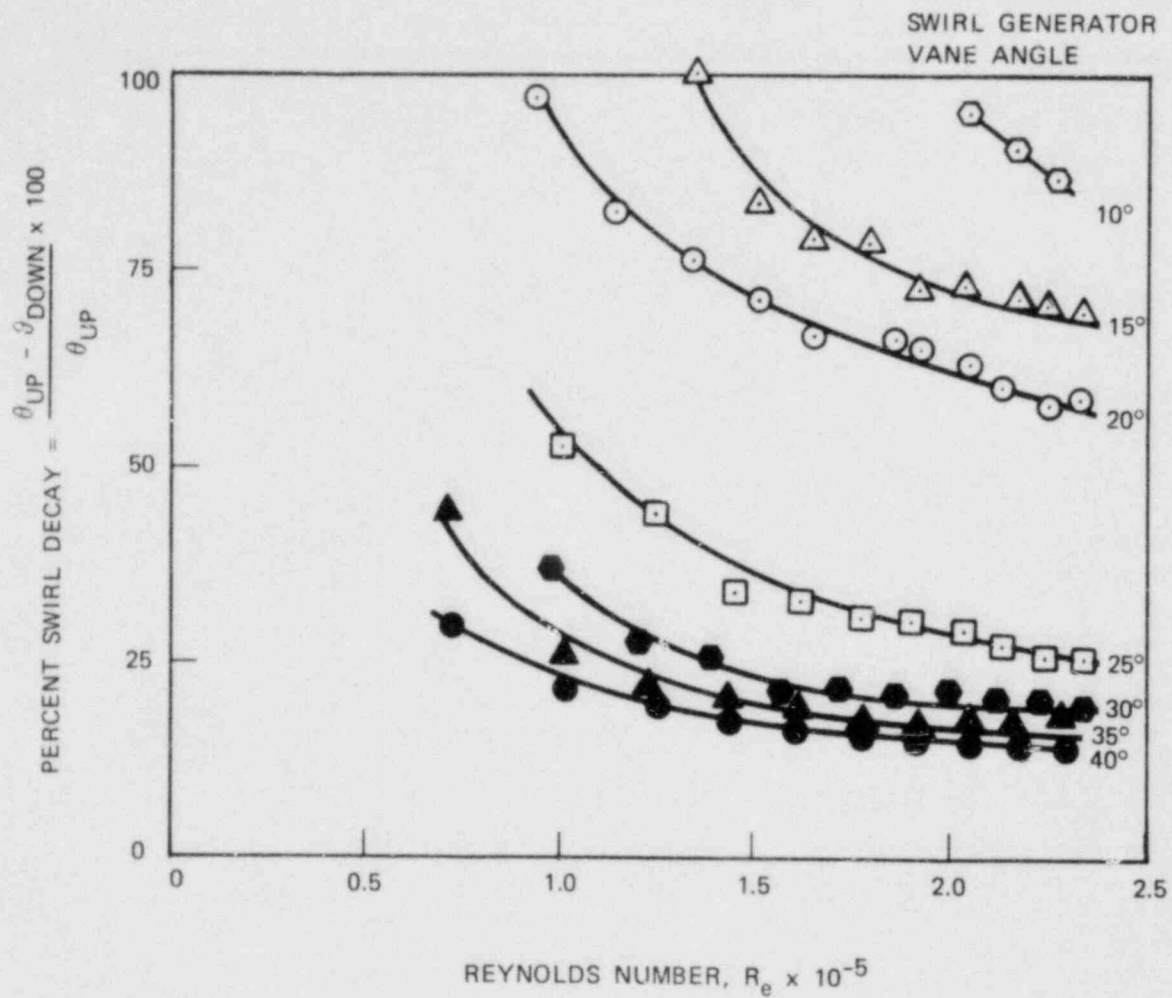


FIGURE 7 SWIRL DECAY OVER 17 PIPE DIAMETERS VERSUS REYNOLDS NUMBER

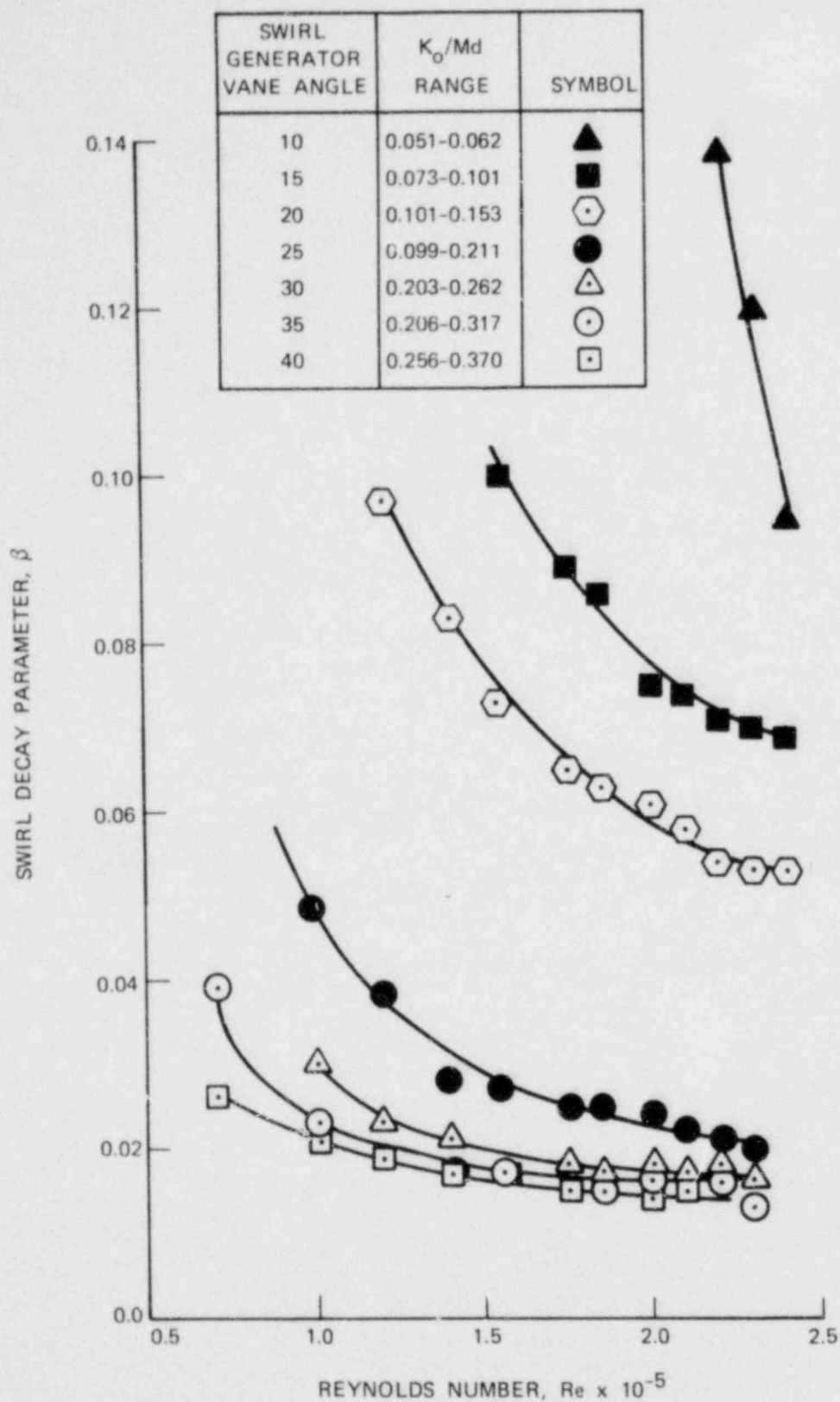


FIGURE 8 β VERSUS REYNOLDS NUMBER FOR SET SWIRL GENERATOR VANE ANGLES AND K_o/Md RANGES



WORCESTER
POLYTECHNIC
INSTITUTE

ALDEN RESEARCH LABORATORY
HOLDEN, MASSACHUSETTS 01520